INTERNATIONAL JOURNAL FOR NUMERICAL METHODS IN FLUIDS
Int. J. Numer. Meth. Fluids 2008; **56**:2021–2043
Published online 29 August 2007 in Wiley InterScience (www.interscience.wiley.com). DOI: 10.1002/fld.1585

Simple efficient algorithm (SEA) for shallow flows with shock wave on dry and irregular beds

Alireza Zia*,†,‡ and Mohamad Ali Banihashemi§

Faculty of Civil Engineering, School of Engineering, University of Tehran, P.O. Box 11365-4563, Tehran, Iran

SUMMARY

An explicit Godunov-type solution algorithm called SEA (simple efficient algorithm) has been introduced for the shallow water equations. The algorithm is based on finite volume conservative discretisation method. It can deal with wet/dry and irregular beds. Second-order accuracy, in both time and space, is achieved using prediction and correction steps. A very simple and efficient flux limiting technique is used to equip the algorithm with total variation dimensioning property for shock capturing purposes. In order to make sure about the balance between the flux gradient and the bed slope, treatment of the source term has been done using a new procedure inspired mainly by the physical rather than mathematical consideration. SEA has been applied to one-dimensional problems, although it can equally be applied to multi-dimensional problems. In order to assess the capability of proposed algorithm in dealing with practical applications, several test cases have been examined. Copyright © 2007 John Wiley & Sons, Ltd.

Received 27 March 2007; Revised 30 June 2007; Accepted 3 July 2007

KEY WORDS: finite volume; shallow flows; Godunov-type solution; approximate Riemann solver; HLLC; dam break; TVD; shock capturing; wet/dry interface; irregular bed; source term

1. INTRODUCTION

Shock capturing techniques in the framework of finite volume discretisation, especially Godunov-type methods, have recently drawn more attentions. Introducing new approximate Riemann solvers and generalization of Godunov's first-order method to the second-order accuracy are considered as two significant developments. Although two-dimensional approximate Riemann solvers have been introduced [1], it is still common to use one-dimensional solvers.

A wide variety of one-dimensional approximate Riemann solvers have been proposed which can be applied more economically than the exact Riemann solver and yet give equally good results

*Correspondence to: Alireza Zia, Faculty of Civil Engineering, School of Engineering, University of Tehran, P.O. Box 11365-4563, Tehran, Iran.
†E-mail: alireza.zia@gmail.com
‡Ph.D. Candidate.
§Assistant Professor.

in many cases. Approximate Riemann solvers can be categorized as two classes [2]. In one class, an approximate solution to the conservative variables will be obtained first, and then flux values will be calculated. The recent work of Julien *et al.* [3] belongs to this class. Another class directly gives an approximate value for the flux function. In this paper, this type of approximate Riemann solver has been used and will be discussed in more detail.

At least five approximate Riemann solvers i.e. Roe, FVS, Osher, HLL and HLLC can be found in the literature, all of which are based on the characteristics theory. The Roe solver is based on a characteristic decomposition of flux differences while ensuring the conservative property [4]. It is not entropy satisfying and it needs an 'entropy fix' in practical applications [4, 5]. Also the Roe solver cannot strictly handle situations involving dry bed states [2, 6] and in fully two-dimensional cases, it seems to give some mono-directionality effects [7]. In the FVS or Flux Vector Splitting method, a key problem is its reliance on special property of the equations, namely the homogeneity property of the flux vector [4, 8], which is not satisfied by the shallow water equations. This may however be circumvented, but it needs some special treatment [9]. Also the FVS is not entropy satisfying [10]. The Osher's scheme uses the Riemann invariants to estimate the flux. It is entropy satisfying with good accuracy. The only shortcoming is its complexity. Zhao *et al.* [9] studied the Osher, Roe and FVS solvers and concluded that the Osher's scheme is the most accurate, the FVS is the most numerically stable with respect to dx and dt variations and the Roe solver is the most stable for bed-level variations.

The HLL approach has been introduced by Harten, Lax and van Leer [11]. The central idea is to assume a wave configuration for the solution that consists of two waves separating three constant states. This assumption is correct only for hyperbolic systems of two equations, such as one-dimensional shallow water equations. For larger systems, the two-wave assumption is not correct. As a consequence, the resolution of physical features, such as contact surface, shear waves and material interface, can be very inaccurate [8]. Also in floods where there is a wet/dry interface, it is important to model the contact wave properly, otherwise a spurious shock front will be predicted [12].

In view of the shortcoming of the HLL approach, a modification called HLLC Riemann solver, in which C stands for Contact, was put forward by Toro *et al.* [13]. HLLC offers successful approximation for practical applications. Both HLL and HLLC provide entropy-satisfying results [5], and their implementation is also easy. Also the HLL and HLLC handle dry-bed situations automatically, provided the wave speed is chosen appropriately [14]. Some authors complained about diffusivity of the HLL and HLLC [15, 16]. In [17], 20 explicit conservative schemes have been examined for the solution of the one-dimensional homogeneous shallow water equations. In the conclusion, for the ease of implementation, efficiency and robustness, the HLL(C) and Osher schemes have been recommended for first-order schemes. Also in comprehensive study of [18], the performance of the Roe, FVS, Osher, HLL and HLLC has been evaluated according to five criteria including ease of implementation, accuracy, applicability, simulation time and stability. In the summary of this study, HLL and HLLC were determined as the high-ranked schemes in terms of ease of implementation. Osher and FVS schemes were also ranked first for accuracy and simulation time, respectively. For the applicability and stability all schemes performed identical except the Roe scheme which had few problems in terms of applicability. Finally, it was highlighted that a first-order accurate solution algorithm using either Osher or HLLC schemes can be recommended for the simulation of all kinds of applications.

Based on the above literature review, the HLLC approximate Riemann solver is adopted in this paper for further developments.

DOI: 10.1002/fld

Godunov-type method with any of the above-mentioned approximate Riemann solvers yields a first-order accuracy. In order to achieve second-order accuracy, a number of algorithms have been proposed. van Leer in a series of papers [19, 20] proposed the monotone upstream scheme for conservation laws (MUSCL). Weighted average flux (WAF) is another second-order algorithm which was introduced by Toro [21]. LeVeque [5] added a correction flux to the first-order Godunov method to gain second-order accuracy. Piece-wise linear method [8], generalized Riemann problem [22, 23] and piece-wise parabolic method [24] are other generalizations of Godunov first-order to second-order method. In this paper, the first-order Godunov-type solution using the HLLC is corrected to achieve the second-order accuracy for its application in shallow water flow modeling.

Godunov-type methods are successful in computing the convection fluxes with high level of accuracy. In shallow water equations in addition to the convection terms, there is a source term due to the real topography. Treatment of this source term has a great influence on the final accuracy of the results and several researches have focused on this topic. A simple method for dealing with the source term is the fractional step method, in which the inhomogeneous form of the equations is split into two sets of equations, a homogeneous set and a set of ordinary differential equations. Both the sets are solved individually during computations. This method provides relatively poor solution for steady and quasi-steady problems [8, 18]. With suggestion of linearly reconstructing water surface instead of water depth, Zhou *et al*. [25] introduced surface gradient method (SGM). The SGM is efficient, but is limited to the Godunov-type methods, which require the variable reconstruction step. Nujic [26] proposed to extract the static pressure term from the flux vector and to include it in the bed slope source term. Excluding the pressure term from the flux function will change the characteristics [27] and will cause difficulties in the application of Godunov-type methods. Nujic's method also suffers from a high level of diffusivity for some kinds of flows [7, 28]. Bermudez and Vazquez [29] proposed an upwind method to discretise the bed slope source term. Vazquez-Cendon [30] applied the same idea to solve various shallow water problems. In Hubbard and Navarro [31], the upwind method of [30] was used to make balance between the source term and the flux gradient in flux difference splitting method. Their scheme is rather complex. LeVeque [32] proposed a treatment to balance the source term and the flux gradient, which works well for quasi-steady problems, but is difficult to be applied to steady transcritical flow with shock. Rogers *et al*. [33, 34] suggested mathematical balancing between the flux gradient and the source term prior to the use of a numerical method. However, neglecting or adding any term will cancel the mathematical balancing. Two methods have been proposed by Mohammadian and Le Roux [28] to treat the source term on unstructured grids. Valiani and Begnudelli [35] proposed DFB (divergence form for bed slope) method to write the bed slope source term in divergence form. The DFB is independent of any discretisation technique. They applied their scheme just for structured grids. Marche *et al*. [36] developed a model which is especially designed for the simulation of wave transformations over strongly varying topography. The influence of the source term on stability, accuracy and conservation in shallow flow simulations has been investigated by Murrilo *et al*. [37] using triangular finite volumes.

The utility of a numerical algorithm for the shallow water equations depends on its ability to deal with various difficulties arising in applications. Since these equations admit shocks, an algorithm should be able to accurately capture moving jump discontinuities. Many applications have realistic arbitrary topography and regions of the domain that are sometimes dry and sometimes wet. Consequently, the algorithm should be robust enough to deal with the appearance or preexistence of dry states, while at the same time handles a reasonably wide range of bottom topographies. Considering these requirements, a high-resolution Godunov-type algorithm is presented in this

DOI: 10.1002/fld

paper. It is a new extension of the first-order Godunov-type method to second-order accuracy and is much simpler than the previous algorithms. The presented algorithm has given satisfactory results for the already mentioned required conditions in one dimension. Complete details are presented in the following sections.

2. GOVERNING EQUATIONS

The governing equations of one-dimensional unsteady flow in a channel of prismatic rectangular cross-section with a sufficient small bottom slope are the Saint Venant equations. These equations express conservation of mass and momentum. In conservative form, they are as follows:

$$U_t + F(U)_x = S$$

$$U = \begin{bmatrix} h \\ hu \end{bmatrix}, \quad F(U) = \begin{bmatrix} hu \\ hu^2 + \frac{1}{2}gh^2 \end{bmatrix}, \quad S = \begin{bmatrix} 0 \\ gh(s_0 - s_f) \end{bmatrix} \tag{1}$$

where U is the conservative variables vector in which, h and u are flow depth and velocity, respectively; $F(U)$ the flux vector; S the source term vector, consist of bed slope S_0 and friction slope S_f.

The friction slope S_f is assumed to be given by the Manning equation:

$$S_f = \frac{n^2 u|u|}{h^{1.33}} \tag{2}$$

where n is the empirical Manning resistance coefficient.

The governing equations are based on the assumptions of hydrostatic pressure distribution, incompressibility of water and a sufficiently small channel slope. In spite of the strong simplifying assumptions, the numerical solution of the equations still remains a computationally challenging task. This is, in the main, due to the hyperbolic character of the equations, which admit discontinuous solution such as shocks, contact discontinuities and shear waves.

3. SOLUTION ALGORITHM

As mentioned in Section 1, a new Godunov-type algorithm for the numerical simulation of shallow water equations is presented in this paper. The algorithm is a two-step predictor–corrector scheme. Both steps are based on the finite volume conservative numerical integration, which results in a second-order accurate scheme, in both space and time.

3.1. Prediction step

The explicit conservative discretised finite volume formula corresponding to Equation (1) is expressed as

$$U^{n+1} = U^n - \frac{\Delta t}{\Delta x}[F_{i+1/2} - F_{i-1/2}]^n + S^n \Delta t \tag{3}$$

where $F_{i\pm 1/2}$ represents the fluxes through the left and right cell interfaces; Δt and Δx are the time step and grid size, respectively; and 'n' denotes the time level.

DOI: 10.1002/fld

In finite volume method, the key problem is the estimation of the normal flux through each side of a cell [9]. There are several schemes to estimate this flux. At the prediction step of the proposed algorithm, the fluxes are computed using the HLLC approximate Riemann solver. In one-dimensional shallow water equation, the resulting fluxes from the HLL or HLLC are identical. When additional equations due to sediment or pollutant transport are added, the HLLC results are more accurate. Thus for the sake of completeness, HLLC method is selected in the proposed algorithm.

In the prediction step, the conservative variables, $\overline{U}$, are calculated using the following formula:

$$\overline{U} = U^n - \frac{\Delta t}{\Delta x}[F^p_{i+1/2} - F^p_{i-1/2}] + S^n \Delta t \tag{4}$$

where $F^p_{i\pm 1/2}$ denotes the flux of the prediction step, $F^p_{i\pm 1/2} = F^{\mathrm{HLLC}}$ and $S^n = S(U^n)$.

Based on [2], the numerical flux of HLLC, F^{HLLC}, is evaluated as follows:

$$F^{\mathrm{HLLC}} = \begin{cases} F_L & \text{if } 0 \leqslant S_L \\ F_{*L} & \text{if } S_L \leqslant 0 \leqslant S_M \\ F_{*R} & \text{if } S_M \leqslant 0 \leqslant S_R \\ F_R & \text{if } 0 \geqslant S_R \end{cases} \tag{5}$$

where $F_L = F(U_L)$, $F_R = F(U_R)$, U_L and U_R are the left and right Riemann states of a local cell interface, respectively; F_{*L} and F_{*R} are the numerical fluxes in the left and right sides of the star region of the Riemann solution which is divided by a shear (contact) wave; and S_L, S_M and S_R are the speeds of the left, shear (contact) and right waves, respectively. In Figure 1, the wave structure assumption of the HLLC is depicted.

The flux vectors F_{*L} and F_{*R} are expressed as

$$F_{*L} = \begin{bmatrix} F^1_* \\ F^2_* \\ F^1_* \cdot \psi_L \end{bmatrix}, \quad F_{*R} = \begin{bmatrix} F^1_* \\ F^2_* \\ F^1_* \cdot \psi_R \end{bmatrix} \tag{6}$$

where Ψ_L and Ψ_R are the left and right initial values of a local Riemann problem for the pollutant/sediment concentration (see Figure 1), and F^1_* and F^2_* are calculated using the HLL

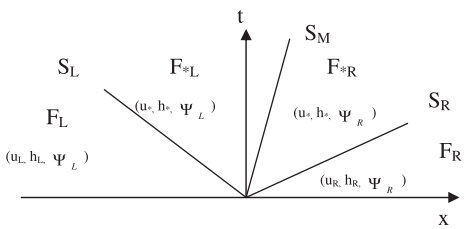

Figure 1. HLLC assumption for wave structure of the Riemann problem solution.

DOI: 10.1002/fld

formula given by Harten *et al*. [11],

$$F_* = \frac{S_R F_L - S_L F_R + S_L S_R (U_R - U_L)}{S_R - S_L} \tag{7}$$

Key to the success of HLLC approach is in identifying the correct wave speeds; S_L, S_M and S_R [14]. For shallow water equations, there are several possible choices. Fraccarollo and Toro [14] recommend the use of two-rarefaction assumption for S_L and S_R. Toro [2] introduced new wave speeds that are robust when there is a shock wave. In the presence of rarefaction wave, the new speeds are the same as the characteristic speeds. For non-linear systems, the characteristic speeds may be distinct from wave speeds. Therefore, it would be desirable to use the two rarefactions assumption for wave speeds when there is a rarefaction wave, and Toro's suggestion in the presence of a shock wave. This idea has been adapted in this paper. By simultaneously considering the dry-bed problem, the speeds can be given as follows:

$$\begin{aligned} S_L &= u_L - \sqrt{g h_L} q_L \\ S_R &= u_R + \sqrt{g h_R} q_R \end{aligned} \quad \text{if } h_* > h_k \text{ (shock wave)} \tag{8}$$

$$\begin{aligned} S_L &= \min(u_L - \sqrt{g h_L}, u_* - \sqrt{g h_*}) \\ S_R &= \max(u_R + \sqrt{g h_R}, u_* + \sqrt{g h_*}) \end{aligned} \quad \text{if } h_* \leqslant h_k \text{ (rarefaction wave)}$$

$$\begin{aligned} S_L &= u_R - 2\sqrt{g h_R} \text{ (for } h_L = 0) \\ S_R &= u_L + 2\sqrt{g h_L} \text{ (for } h_R = 0) \end{aligned} \quad \text{if } h_k = 0 \text{ (dry bed)}$$

$$S_M = \frac{S_L h_R (u_R - S_R) - S_R h_L (u_L - S_L)}{h_R (u_R - S_R) - h_L (u_L - S_L)} \tag{9}$$

$q_k (k = L, R)$ is given by

$$q_k = \sqrt{\frac{1}{2}\left[\frac{(h_* + h_k) h_*}{h_*^2}\right]} \tag{10}$$

where u_L, u_R, h_L and h_R are left and right initial values for a local Riemann problem, and u_* and h_* are calculated from

$$u_* = \tfrac{1}{2}(u_L + u_R) + \sqrt{g h_L} - \sqrt{g h_R} \tag{11}$$

$$h_* = \frac{1}{g}\left[\frac{1}{2}\left(\sqrt{g h_L} + \sqrt{g h_R}\right) + \frac{1}{4}(u_L - u_R)\right]^2 \tag{12}$$

Treatment of the source term and the proposed method to computing S^n will be discussed in Section 4.

3.2. Correction step

Without solving Riemann problem, the fluxes are calculated using Riemann problem states, i.e. cell interface values of predicted variables. In contrast to the prediction step in which the flux values were obtained in an upwind manner using the HLLC solver, correction fluxes are obtained

DOI: 10.1002/fld

in the downwind direction by direct evaluation of the flux vector. The discretised form of governing equations after the correction step takes the following form:

$$U^{n+1} = U^n - \frac{\Delta t}{\Delta x}[F_{i+1/2} - F_{i-1/2}] + S\Delta t \tag{13}$$

$$F_{i\pm1/2} = \tfrac{1}{2}[F^p_{i\pm1/2} + F^c_{i\pm1/2}]$$

$$F^c_{i+1/2} = \begin{cases} F(\overline{U}^R_{i+1/2}) & \text{if } u_i \geqslant 0 \\ F(\overline{U}^L_{i+1/2}) & \text{if } u_i < 0 \end{cases} \tag{14}$$

$$S = \tfrac{1}{2}(S^n + S^p), \quad S^n = S(U^n), \quad S^p = S(\overline{U}) \tag{15}$$

where U^{n+1} represents the conservative variables at new time step $(n+1)$; $F^c_{i\pm1/2}$ the correction step fluxes; $F_{i\pm1/2}$ the final flux values; $\overline{U}^R_{i+1/2}/\overline{U}^L_{i+1/2}$ the predicted value of conservative variable at right/left side of $i + \frac{1}{2}$ cell interface and S^n/S^p the source term evaluated using the previous time step/predicted values of conservative variables.

4. TREATMENT OF THE SOURCE TERM

The treatment of the source term has an important role in the final accuracy of the results. The source term consists of two parts, the bed slope and the friction slope. Treatment of each part will be explained separately.

4.1. Bed slope treatment

The main subject in dealing with the bed slope is to balance it with the convection flux in each cell at stationary flow field. This will be explained in more detail under the C-property preposition [29]. The C-property will be explained and approved for the proposed algorithm later on, but first the details of the source term discretization are presented below.

Implementing a staggered grid idea, the bed elevation is assigned to each cell interface and a linear variation is assumed inside each cell (see Figure 2).

According to the definition sketch of Figure 2,

$$\eta = h + z \tag{16}$$

where η is the water surface elevation, h the water depth and z the bed elevation.

With the assumption of no erosion and no sedimentation ($\partial z/\partial t = 0$) one would obtain the following equation:

$$\frac{\partial \eta}{\partial t} = \frac{\partial h}{\partial t} \tag{17}$$

Using Equation (17), the continuity equation takes the form:

$$\frac{\partial \eta}{\partial t} + \frac{\partial hu}{\partial x} = 0 \tag{18}$$

DOI: 10.1002/fld

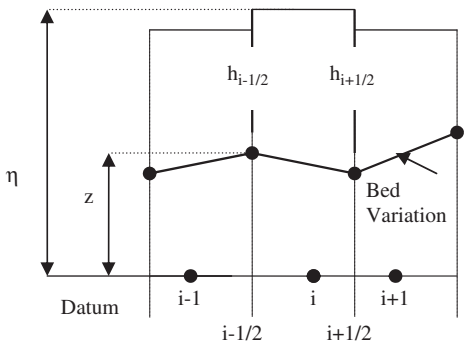

Figure 2. Definition sketch for bed slope.

The bed slope term for cell i, S_{1i}, could be rewritten as follows:

$$S_{1i} = g h_i S_{0i} \tag{19}$$

S_{0i} is the bed slope of cell i and $S_{0i} = -\partial z/\partial x|_i$. Regarding Figure 2, $z = \eta - h$; therefore,

$$-\frac{\partial z}{\partial x} = \frac{\partial h}{\partial x} - \frac{\partial \eta}{\partial x} \tag{20}$$

Assuming a constant water level inside each cell, i.e. $\partial\eta/\partial x|_i = 0$, Equation (20) simplifies to: $-\partial z/\partial x = \partial h/\partial x$. Thus, S_{0i} can be rewritten as $S_{0i} = \partial h/\partial x|_i$; therefore,

$$S_{0i} = \frac{h_{i+1/2} - h_{i-1/2}}{\Delta x} \tag{21}$$

Using Equation (21) and also $h_i = (h_{i+1/2} + h_{i-1/2})/2$, Equation (19) becomes

$$S_{1i} = \frac{0.5g(h_{i+1/2} + h_{i-1/2})(h_{i+1/2} - h_{i-1/2})}{\Delta x} \tag{22}$$

C-property proposition
In the presence of a stationary flow field, if a numerical method could preserve the conservative property, then it satisfies the exact C-property.

For each step of proposed algorithm, the C-property is investigated separately.

4.1.1. Prediction step. Using the HLLC solver, the following relations stand in the stationary flow field case:

$$u = 0, \quad hu = 0 \tag{23}$$

$$\begin{aligned} S_L &= -\sqrt{g h_L} < 0 \\ S_R &= \sqrt{g h_R} > 0 \end{aligned} \tag{24}$$

DOI: 10.1002/fld

Using Equation (7), the predicted flux for the interface $i+\frac{1}{2}$ with respect to Equations (23) and (24) can be rewritten as follows:

$$F^p_{i+1/2} = \frac{\sqrt{gh_R}(0.5gh_L^2) - (-\sqrt{gh_L}(0.5gh_R^2))}{\sqrt{gh_R}+\sqrt{gh_L}} \tag{25}$$

For interface $i+\frac{1}{2}$ at stationary flow field: $h_R = h_L = h_{i+1/2}$, thus Equation (25) is simplified to

$$F^p_{i+1/2} = 0.5gh^2_{i+1/2} \tag{26}$$

If the same procedure is repeated for the flux through the interface $i-\frac{1}{2}$, it can be written as

$$F^p_{i-1/2} = 0.5gh^2_{i-1/2} \tag{27}$$

Replacing Equations (22), (26) and (27) by the discretised form of governing equations, i.e. Equation (4), results in

$$\overline{hu}_i = hu^n_i - \frac{\Delta t}{\Delta x}[0.5gh^2_{i+1/2} - 0.5gh^2_{i-1/2}] + \frac{0.5g\Delta t}{\Delta x}[h^2_{i+1/2} - h^2_{i-1/2}] \tag{28}$$

The second and third terms on right-hand side of Equation (28) cancel each other; hence,

$$\overline{hu}_i = hu^n_i \tag{29}$$

Equation (29) approves the conservative property, hence satisfying the exact C-property of the prediction step.

4.1.2. Correction step. In the proposed algorithm, the correction fluxes are obtained in downwind manner. If the convection fluxes for interfaces $i+\frac{1}{2}$ and $i-\frac{1}{2}$ in the momentum equation are computed and replaced in the discretised form of governing equations, the following relation will be obtained:

$$hu^{n+1}_i = hu^n_i \tag{30}$$

It is concluded, therefore, that the proposed algorithm satisfies the exact C-property in both prediction and correction steps.

4.2. Friction slope treatment

Lack of spatial derivatives in this part of the source term makes its implementation easy. Using conservative variables h, hu and Manning's formula, the friction slope can be written as

$$S_f = \frac{n^2 hu|hu|}{h^{10/3}}$$

$$(S_f)_i = \frac{n^2 (hu)_i |hu|_i}{h_i^{10/3}} \tag{31}$$

DOI: 10.1002/fld

5. SHOCK CAPTURING TECHNIQUE

Considering the numerical phenomenon, which may result in generation of spurious oscillations, a systematic analysis of the conditions required by a scheme to achieve oscillation free results has been developed. Godunov [38], who introduced the important concept of monotonicity, proved rigorously that numerical oscillations are unavoidable if one uses linear methods of accuracy greater than 1 [4].

Solutions to conservation laws, which contain shocks and contact discontinuities, are not uniquely determined by their initial values. The physically relevant solution from the set of weak solutions must also satisfy the entropy conditions [4, 8]. Weak solutions are the set of solutions which satisfy both the Rankine–Hugoniot jump condition and the governing equations. For an arbitrary flux function $F(U)$, the following relationship between the shock speed S and the states U_L and U_R across the shock is called the Rankine–Hugoniot jump condition:

$$F(U_L) - F(U_R) = S(U_L - U_R) \tag{32}$$

The entropy condition simply ensures that shocks are only formed when characteristics converge. Violation of this condition will result in the non-physical rarefaction shock or an expansion shock [4, 17].

Monotone schemes satisfy all the above conditions, but according to Godunov [38], monotone schemes are only first order. This represents a sever limitation, since first-order accuracy is insufficient for practical purposes, the corresponding scheme being too diffusive. Hence, conditions less severe than monotonicity have to be defined to allow the definition of schemes with an accuracy higher than one which generate entropy satisfying solutions without overshoots at shock and contact discontinuities. Schemes of this type are called high-resolution schemes [4].

The keynote of above-mentioned Godunov's theorem is to have desirable results one must use non-linear method even when applied to linear problem [2, 4]. This important concept has been introduced initially by van Leer [39], Boris and Book [40] and then by Sweby [41] under the form of limiters, which control the gradients of over or under shoots. Using limiters, the total variation dimensioning (TVD) condition will be provided, which is a weaker condition than monotonicity [42]. TVD is more general than monotonicity, but this condition does not ensure satisfaction of the entropy condition. Godunov-type methods will always satisfy entropy condition provided that the Riemann solution used to define the flux at each cell interface satisfies the entropy condition [5]. In TVD technique, the solution of governing equations near the shocks or discontinuities will be of first order, while in the smooth region it has second-order accuracy. Switching from second order to first order and *vice versa* will be done using appropriate limiters. Limiters could be categorized as two groups, slope and flux limiters.

ENO (essentially non-oscillatory scheme) and WENO (weighted essentially non-oscillatory scheme) are other attractive techniques for shock capturing.

Methodology for the definition of a second-order high-resolution TVD scheme in the proposed algorithm is to restrict a part of the numerical flux. A similar approach has been used by Yu and Liu [43] and then by Lin *et al.* [44] in conjunction with flux vector splitting method. Utilizing the flux limiter, a very simple approach is used for shock capturing. The flux in Equation (13) can be rewritten as

$$F_{i\pm1/2} = \tfrac{1}{2}[F^p_{i\pm1/2} + F^c_{i\pm1/2}]$$

DOI: 10.1002/fld

$$F_{i\pm1/2} = F^p_{i\pm1/2} + \tfrac{1}{2}[F^c_{i\pm1/2} - F^p_{i\pm1/2}]$$

$$F^{\mathrm{TVD}}_{i\pm1/2} = F^p_{i\pm1/2} + \tfrac{1}{2}\varphi(r)[F^c_{i\pm1/2} - F^p_{i\pm1/2}] \tag{33}$$

where $F^{\mathrm{TVD}}_{i\pm1/2}$ is the high-resolution flux i.e. TVD flux, φ the flux limiter function and r the flux gradient ratio.

Several options are available for the flux limiter such as Superbee and Minmod functions which are as follows:

$$\text{(a) Superbee:} \quad \varphi(r) = \max[0; \min(2r, 1); \min(r, 2)] \tag{34}$$

$$\text{(b) Minmod:} \quad \varphi(r) = \max[0; \min(1, r)] \tag{35}$$

In addition to suppress the numerical oscillations, another advantage of using limiters is that phase error can be essentially eliminated [5]. The argument r is the ratio of the upwind variation to the local variation of flux, $r = \Delta_{\mathrm{upw}}/\Delta_{\mathrm{loc}}$. For cell interface $i + \frac{1}{2}$:

$$r_{i+1/2} = \begin{cases} \dfrac{F^c_{i-1/2} - F^p_{i-1/2}}{F^c_{i+1/2} - F^p_{i+1/2}} & \text{if } u^n_i \geqslant 0 \\ \dfrac{F^c_{i+3/2} - F^p_{i+3/2}}{F^c_{i+1/2} - F^p_{i+1/2}} & \text{if } u^n_i < 0 \end{cases} \tag{36}$$

6. BOUNDARY CONDITIONS

According to the theory of characteristics, two physical boundary conditions, one at the upstream end and another at the downstream end, are needed when the flow regime is subcritical. Remaining unknown parameters at each boundary can be computed using Riemann invariants [45]. For supercritical flow, these two boundary conditions are needed at the upstream end. Without considering the flow regime, two types of boundary conditions can be imposed. These are open or transmissive and close or reflective boundaries. In the first case, the velocity and depth in the boundary ghost cells will be equal to the first grid values inside the computational domain [4]:

$$\begin{aligned} h_0 &= h_1, \quad h_{n+1} = h_n \\ u_0 &= u_1, \quad u_{n+1} = u_n \end{aligned} \tag{37}$$

where the subscript 0 denotes the ghost cell out of the computational domain. For a close or reflective boundary,

$$\begin{aligned} h_0 &= h_1, \quad h_{n+1} = h_n \\ u_0 &= -u_1, \quad u_{n+1} = -u_n \end{aligned} \tag{38}$$

DOI: 10.1002/fld

7. STABILITY CRITERION

The foregoing numerical scheme is explicit, and its stability is governed by the Courant–Friedrichs–Lewy (CFL) criterion. For a one-dimensional grid, the CFL criterion for choosing an appropriate time step Δt may be expressed as

$$\Delta t = Cr \cdot \min\left[\frac{\Delta x_i}{|u_i| + \sqrt{g h_i}}\right] \tag{39}$$

where Cr is the Courant number specified in the range $0 < Cr \leqslant 1$.

8. EVALUATION OF ALGORITHM

To evaluate the performance of the proposed algorithm to solve both steady and unsteady flows, some test cases have been taken from literature. To make reasonable comparison between the calculated results and the published data, similar numerical requirements such as Courant number and number of grids have been established.

The test cases are categorized as two groups. At first, problems with horizontal frictionless bed are examined to assess the capability of the algorithm in dealing with convection terms. Then test cases with source terms due to the irregular and rough beds are used to evaluate another important characteristic of the algorithm.

8.1. Problems with horizontal and frictionless bed

Several flux limiters have been used for this group of test cases. It was observed that the application of Minmod in conjunction with the proposed simple efficient algorithm (SEA) yields better results, and thus these results are presented.

8.1.1. One-dimensional dam break on a frictionless bed. Several authors have used this test in the literature to assess the shock capturing ability of their algorithm. In this test, a vertical wall separating water in a unit width channel with upstream depth of 5 m and a downstream depth of 0.3 m is removed instantaneously. The computational time step and grid size are 0.05 s and 1 m, respectively. The resulting water surface profile and velocity distribution 10 s after dam failure are shown in Figure 3(a) and (b), along with the analytical solution of the problem. To make comparison between the proposed algorithm and the other well-developed schemes, in Figure 3(c) and (d) the same results with the same time step and computational cell size are presented, which have been taken from [18]. These results have been obtained using two second-order accurate schemes, i.e. MUSCL and a prediction–correction, both with the Osher approximate Riemann Solver. Based on these results, good shock capturing skills can be assigned for the proposed algorithm.

8.1.2. Left critical rarefaction and right shock. The next four tests have been designed by Toro [2]. In all tests, the computational domain is a channel of 50 m long, unit width frictionless and horizontal bed. The specifications of each test included in Table I where h_L, h_R, u_L and u_R are depth and velocity in the left and right side of x_0 which is the position of initial discontinuity, and t_{out} is the output time. Analytical solutions have been taken from [2]. Also the numerical results using WAF with HLLC have been presented in [2], but only for the test cases 8-1-2 and 8-1-3;

DOI: 10.1002/fld

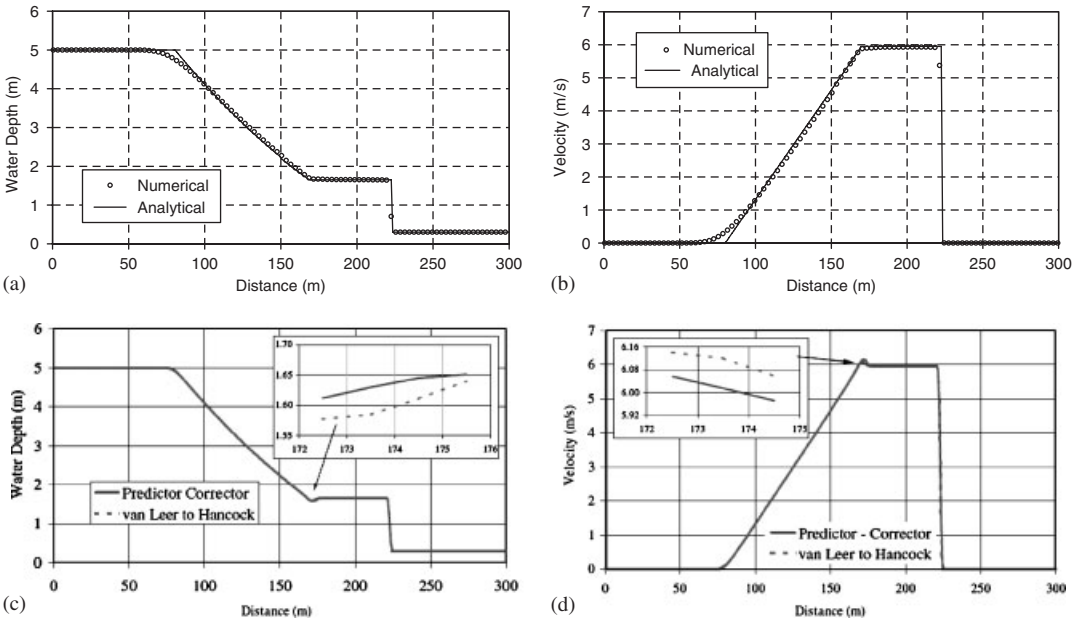

Figure 3. One-dimensional dam break on a frictionless bed: (a), (c) water depth and (b), (d) velocity. (a), (b) Present work and (c), (d) from [18] using MUSCL and predictor–corrector schemes both with Osher approximate Riemann solver.

Table I. Specifications of tests (8-1-2)–(8-1-5).

Test no.	h_L (m)	u_L (m/s)	h_R (m)	u_R (m/s)	x_0 (m)	t_{out} (s)
8-1-2	1.0	2.5	0.1	0.0	10	7.0
8-1-3	1.0	−5.0	1.0	5.0	25	2.5
8-1-4	0.0	0.0	1.0	0.0	30	4.0
8-1-5	0.1	−3.0	0.1	3.0	25	5.0

therefore, the comparison has been made for these two tests. Similar to [2], all tests have been run with $Cr = 0.9$ and 100 cells.

The initial data for test 8-1-2 cause a strong right propagating shock wave and a critical left rarefaction wave. The results are presented in Figure 4(a). Items to check are (a) correct speed of propagation, (b) correct strength of jump, (c) width of shock layer and (d) absence of spurious oscillation in the vicinity of the shock [2]. The agreement between the numerical and analytical results is good. Figure 4(b) shows the WAF results for this test.

8.1.3. Two rarefactions and nearly dry bed. The solution of this test consists of two strong rarefaction waves traveling in opposite directions. The reason for this test is to examine the ability of the numerical algorithm to deal with very shallow regions produced by strong rarefaction. Such situation may lead to negative depths. The results are shown in Figure 5(a). It is evident that no

DOI: 10.1002/fld

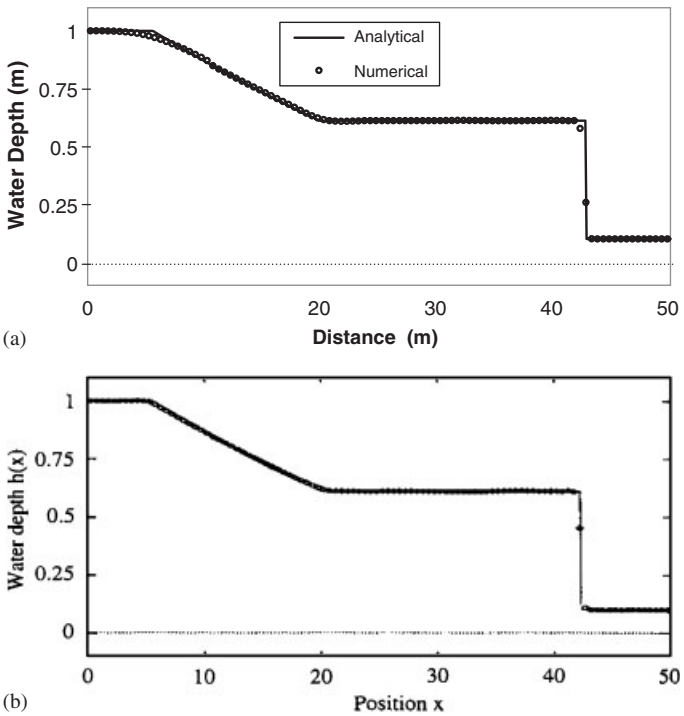

Figure 4. Left critical rarefaction and right shock: water surface profile. (a) Present work and (b) from [2] using WAF and HLLC approximate Riemann solver.

negative depth has appeared. The results obviously show the robustness of proposed algorithm to deal with this kind of problems. Figure 5(b) shows the WAF results for this test.

8.1.4. Dam break problem with downstream dry bed. The downstream section of the dam is dry in this test case. The solution consists of a single right rarefaction wave, with the wet/dry front attached to the tail of it. The propagation of wet/dry front at the correct speed is one major difficulty of numerical methods. In a real application in which such fronts are to be propagated by several kilometers, the propagation speed and thus the predicted wave arrival time will suffer from considerable errors, rendering the prediction unreliable or even useless [2]. Methods based on the assumption that the bed is wet throughout are incorrect for these problems [2]. In Figure 6, the calculated and analytical water surface profiles are shown. Close agreement can be seen. Also a low level of diffusivity can be seen in the rarefaction part of this test.

8.1.5. Appearance of dry region. This test has been designed to produce a dry region in the middle part of computational domain. The aim is to examine the capability of algorithm in dealing with wet/dry fronts traveling in opposite directions. Numerical methods are bound to experience serious difficulties in resolving these conditions [2]. It is seen form Figure 7 that proposed algorithm has good capability in forecasting the appearance of dry region.

DOI: 10.1002/fld

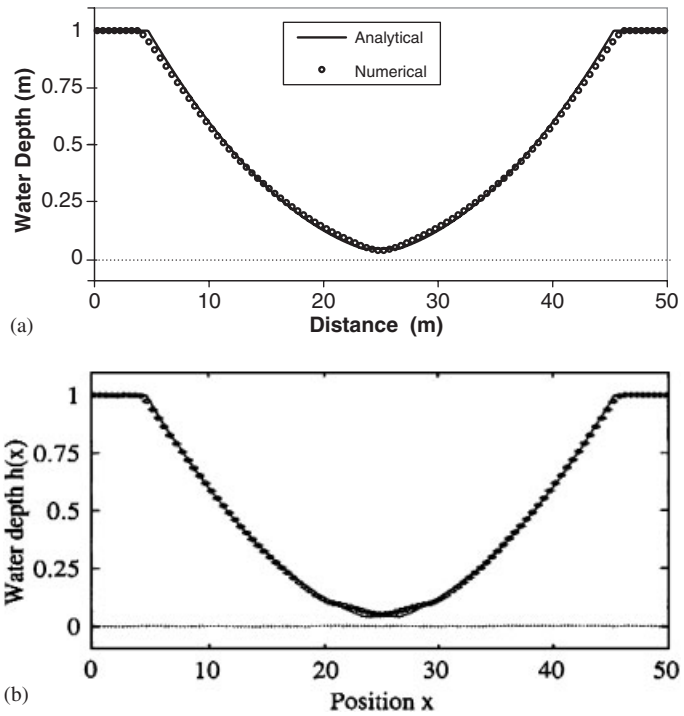

Figure 5. Two rarefactions and nearly dry bed: water surface profile. (a) Present work and (b) from [2] using WAF and HLLC approximate Riemann solver.

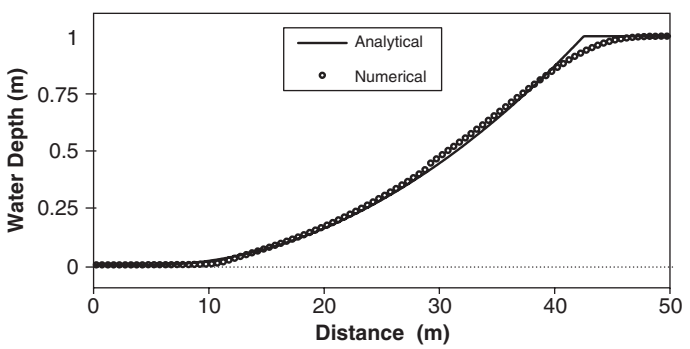

Figure 6. Dam-break problem with downstream dry bed: water surface profile.

8.2. Problems with irregular and rough bed

In test cases 8-2-1 till 8-2-3, the bed slope is just present in the source term. However in test case 8-2-4, the bed and friction slopes are both involved. In contrast with the test cases with horizontal and frictionless bed, these groups of test cases yield better results when in the proposed SEA, the Superbee function is used as a flux limiter.

DOI: 10.1002/fld

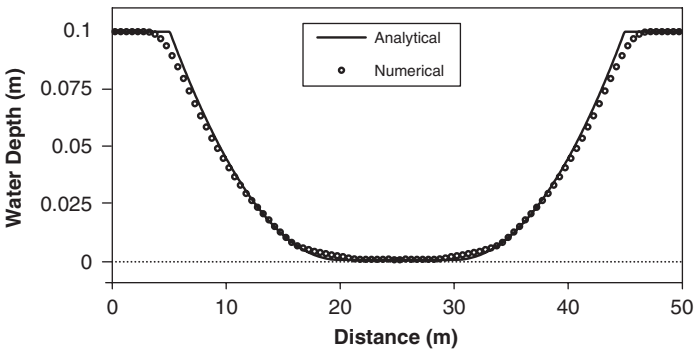

Figure 7. Appearance of dry region: water surface profile.

8.2.1. Tidal wave flow. A test problem originally considered by Bermudez and Vazquez [29] is discussed here. This is a one-dimensional problem with bed topography defined by

$$H(x) = 50.5 - \frac{40x}{L} - 10\sin\left[\pi\left(\frac{4x}{L} - \frac{1}{2}\right)\right]$$

where $L = 14\,000$ m is the channel length. The initial and boundary conditions are

$$\text{ICs} = \begin{cases} h(x,0) = H(x) \\ u(x,0) = 0 \end{cases}$$

$$\text{BCs} = \begin{cases} h(0,t) = H(0) + 4 - 4\sin\left[\pi\left(\dfrac{4t}{86\,400} + \dfrac{1}{2}\right)\right] \\ u(L,t) = 0 \end{cases}$$

With the above conditions, Bermudez and Vazquez [29] derived the following asymptotic analytical solutions:

$$h(x,t) = H(x) + 4 - 4\sin\left[\pi\left(\frac{4t}{86\,400} + \frac{1}{2}\right)\right]$$

$$u(x,t) = \frac{(x-L)\pi}{5400h(x,t)}\cos\left[\pi\left(\frac{4t}{86\,400} + \frac{1}{2}\right)\right]$$

The numerical results of this test case with $\Delta x = 280$ m at $t = 7552.13$ s are presented in Figure 8(a) and (b). These figures show very close agreement between the numerical and analytical solutions. Figure 8(c) and (d) is same as 8(a) and (b), respectively. These results related to MUSCL, with HLL approximate Riemann solver, and SGM for the source term treatment [25].

8.2.2. Steady transcritical flow with a shock over a bump. This benchmark test which has been used by several researchers comprises one-dimensional steady flow in a 25 m long, unit width

DOI: 10.1002/fld

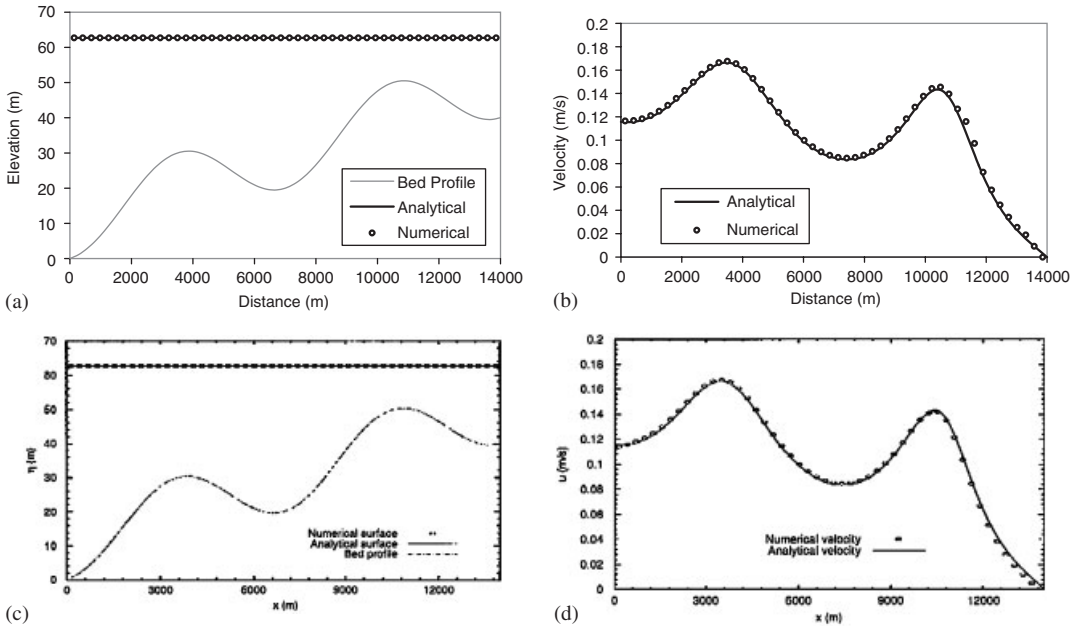

Figure 8. Tidal wave flow: (a), (c) water surface and bed elevation and (b), (d) velocity distribution. (a), (b) Present work and (c), (d) from [25] using MUSCL schemes with HLL approximate Riemann solver and SGM for the treatment of the source term.

channel with a bump defined by

$$Z_b(x) = \begin{cases} 0.2 - 0.05(x-10)^2 & \text{if } 8 < x < 12 \\ 0 & \text{otherwise} \end{cases}$$

where x is the distance along the channel. The goal is to assess the ability of the algorithm to converge to a steady-state solution. This problem was introduced by Goutal and Maurel [46]. Depending on the initial and boundary conditions, the flow may be transcritical with or without a shock, or subcritical. Because it is challenging for a numerical algorithm to predict a steady discontinuous solution over a non-uniform bathymetry, the boundary conditions have been chosen to include transcritical flow with a shock over the bump. Thus, unit discharge of $q = 0.18\,\mathrm{m}^2/\mathrm{s}$ and water depth of $h = 0.33\,\mathrm{m}$ were imposed as an upstream and downstream boundary conditions, respectively. One hundred and fifty computational cells have been used in the computations. It is clearly seen from Figure 9(a) and (b) that the proposed algorithm can provide a solution of accuracy comparable to the analytical results. A low level of oscillation appears in numerical results of discharge. This is the case with all of presented results in the literature even with much more grids, for instance, 200 grids in [25], 256 grids in [34] and 2000×4 grids in a two-dimensional model in [35]. It can be concluded that in the presence of real topography, the C-property does not guarantee that steady-state condition with non-zero discharge will be well captured. This issue has also been reported before by Mohammadian and Le Roux [28]. For comparison, in Figure 9(c)

DOI: 10.1002/fld

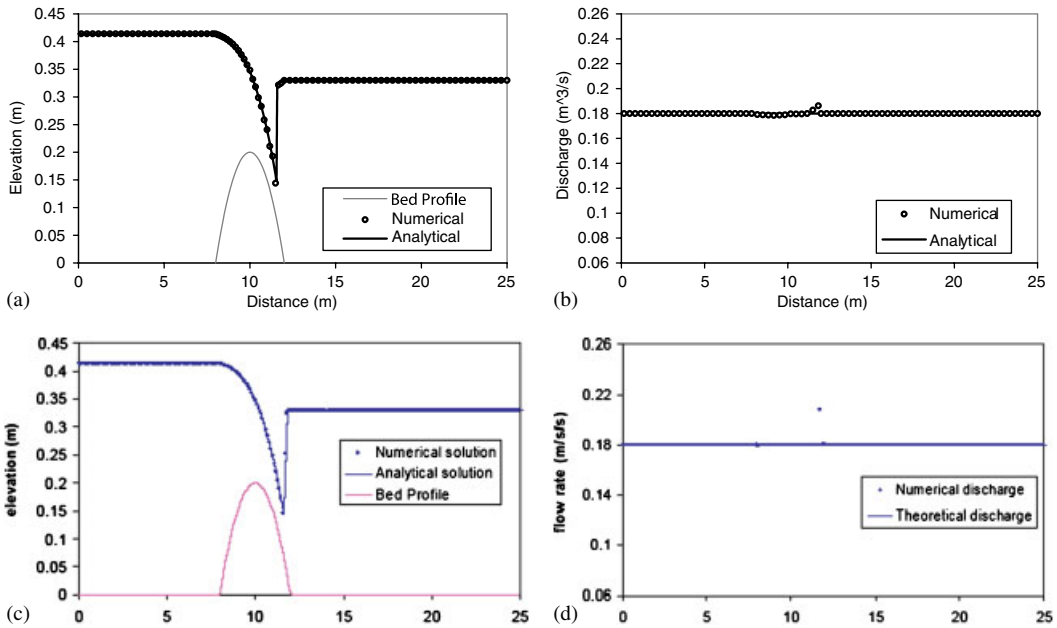

Figure 9. Steady transcritical flow with a shock over a bump: (a), (c) water surface and bed elevation and (b), (d) discharge. (a), (b) Present work and (c), (d) from [34] using MUSCL schemes with Roe approximate Riemann solver and mathematical balancing for the source term.

and (d) the results of [34] are also presented. These results have been obtained using MUSCL schemes with Roe approximate Riemann solver and mathematical balancing of the source term.

8.2.3. Small perturbation of a steady-state solution. This test case has been designed by LeVeque [32]. It was chosen to demonstrate the capability of the proposed algorithm for computations involving small perturbation of the water surface, and to show that the method also works well in the modeling of wave propagation problems. The computational domain is a unit width channel of length 1 m and the bed profile is defined as

$$Z_b = \begin{cases} 0.25[\cos(\pi(x-0.5)/0.1)+1] & \text{if } |x-0.5|<0.1 \\ 0 & \text{otherwise} \end{cases}$$

on $0<x<1$ with $H(0)=1\,\text{m}$ and $g=1\,\text{m/s}^2$. The initial condition was the stationary solution of $u=0\,\text{m/s}$ and

$$\eta(x,0) = \begin{cases} H(0)+\varepsilon & \text{if } 0.1<x<0.2 \\ 0 & \text{otherwise} \end{cases}$$

where ε is the small perturbation in the stationary water surface. Theoretically, this disturbance splits into two waves, propagating left and right. Many numerical methods have difficulty with calculations involving such small perturbations of the water surface [25]. The calculated results for $\varepsilon=0.2\,\text{m}$ and $\varepsilon=0.01\,\text{m}$ at $t=0.7\,\text{s}$ are shown in Figure 10(a) and (b), respectively. The

DOI: 10.1002/fld

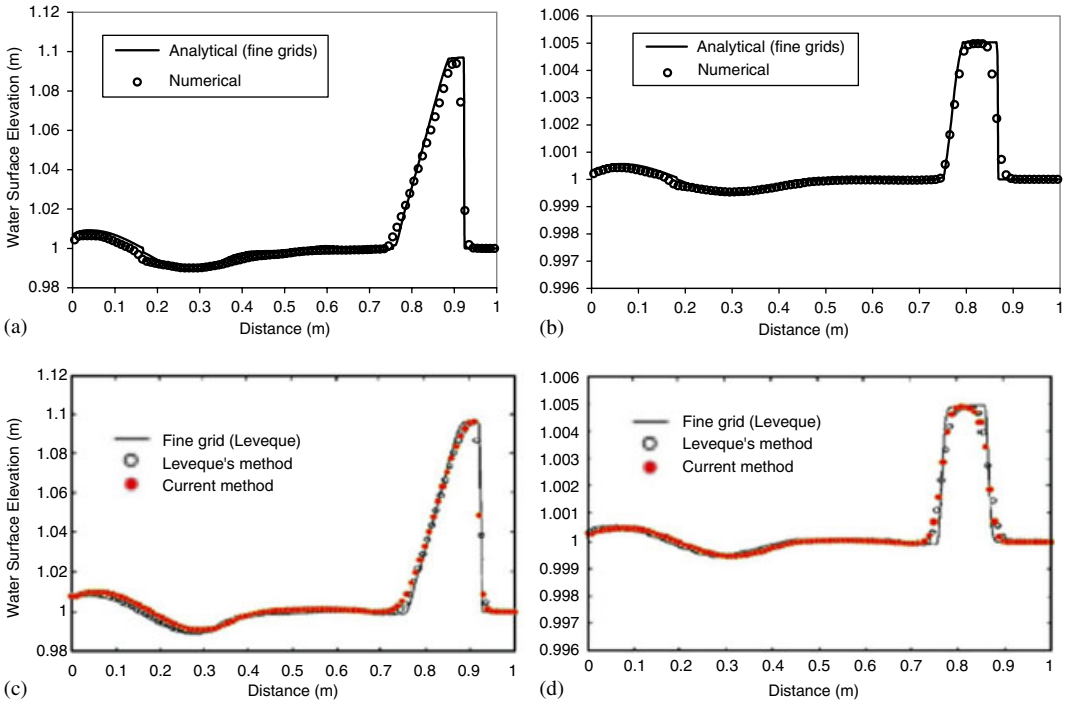

Figure 10. Small perturbation of a steady-state solution: (a), (c) water surface profile for $\varepsilon = 0.2$ m and (b), (d) water surface profile for $\varepsilon = 0.01$ m. (a), (b) Present work and (c), (d) from [15] using MUSCL schemes with Roe approximate Riemann solver.

analytical results are obtained using very fine (2000) grids. Good agreement between numerical and analytical results is achieved. In comparison with some references, which have used too many grids for numerical computation, in the present work, the computational domain has been divided into just 100 cells. The same results using MUSCL and Roe approximate Riemann Solver [15] are shown in Figure 10(c) and (d), for comparison.

8.2.4. Sub-super-sub-critical flow with hydraulic jump. In order to assess the proposed algorithm more realistically, the friction slope of the source term should be incorporated. For this purpose, a test case designed by Mac Donald *et al*. [47] has been selected. The problem has a subcritical inflow and outflow with a supercritical central section. The transition from the subcritical to the supercritical state is carried out through the hydraulic jump. The domain includes a rectangular channel of 100 m long with unit discharge of $2\,\mathrm{m}^2/\mathrm{s}$ and the Manning's roughness coefficient of 0.03. One hundred computational cells have been used. Figure 11(a) represents the comparison between the analytical and numerical results for the water surface. The results confirm the good performance of the proposed algorithm. In Figure 11(b) and (c) the magnified shock region is shown. Figure 11(b) has been obtained using SEA and Figure 11(c) has been taken from [48]. In Figure 11(c), the results of MUSCL and the first-order Roe have been shown. In addition, the result of a second-order scheme, named 'symmetric', is presented in Figure 11(c). All the schemes have a small deviation from analytical solution.

DOI: 10.1002/fld

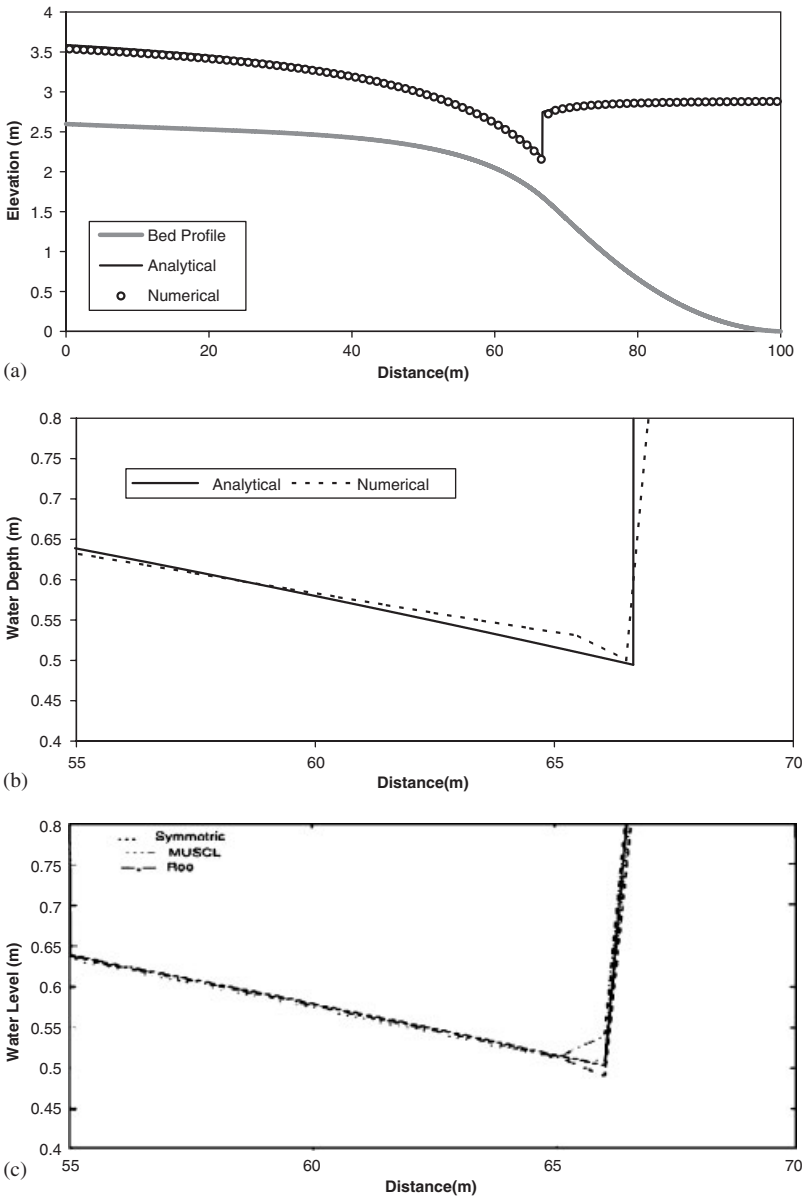

Figure 11. Sub-super-sub-critical flow with hydraulic jump: (a) water surface and bed elevation and (b), (c) magnified shock region. (b) Present work and (c) from [48] using MUSCL and Roe approximate Riemann solver.

DOI: 10.1002/fld

9. CONCLUSION

A new package, which is called SEA, simple efficient algorithm, is proposed for the numerical modeling of non-linear system of shallow water equations. SEA is a Godunov-type solution and is second-order accurate both in time and space. This accuracy has been achieved using a two-step predictor–corrector algorithm. At the prediction step the HLLC Riemann solver is used. The success of the HLLC greatly depends on proper choice of the wave speeds. A new combination of existing relations for the wave speeds is used at the prediction step. At the correction step, the fluxes are easily obtained using the Riemann states without solving the Riemann problem. To consider variable topography, a new simple approach for source term has been proposed which satisfies the C-property in conjunction with the proposed flux computation methods, both in prediction and correction steps. Since the spurious oscillations in second-order schemes are inherent, an efficient flux limiting technique is used to supply TVD property and thus to overcome this defect.

The overall competency of the new algorithm in dealing with various types of problems encountered in hydraulic modeling is assessed by several test cases and compared with well-developed schemes. Main features of the present work are simplicity and efficiency, which are desirable in dealing with complex practical problems.

This work could be a base for a more general two-dimensional model, the result of which would be presented in the near future.

REFERENCES

1. Guinot V. An approximate two-dimensional Riemann solver for hyperbolic system of conservation laws. *Journal of Computational Physics* 2005; **25**(1):292–314.
2. Toro EF. *Shock Capturing Methods for Free Surface Shallow Flows*. Wiley: Chichester, 2001.
3. Julien L, Vincent G. A general approximate-state Riemann solver for hyperbolic systems of conservation laws with source terms. *International Journal for Numerical Methods in Fluids* 2006; **53**(9):1509–1540.
4. Hirsch C. *Numerical Computation of Internal and External Flows*, vol. 2. Wiley: England, U.K., 1990.
5. LeVeque RJ. *Finite Volume Methods for Hyperbolic Problems*. Cambridge University Press: New York, 2002.
6. Caleffi V, Valiani A, Zanni A. Finite volume method for simulating extreme flood events in natural channels. *Journal of Hydraulic Research* 2003; **41**(2):167–177.
7. Valiani A, Caleffi V, Zanni A. Case study: malpasset dam-break simulation using a two-dimensional finite volume method. *Journal of Hydraulic Engineering* 2002; **128**(5):460–472.
8. Toro EF. *Riemann Solvers and Numerical Methods for Fluid Dynamics*. Springer: Berlin, 1999.
9. Zhao DH, Shen HW, Lai JS, Tabios GQ. Approximate Riemann solvers in FVM for 2D hydraulic shock wave modeling. *Journal of Hydraulic Engineering* 1996; **122**(12):692–702.
10. Lin GF, Lai JS, Guo WD. High-resolution TVD schemes in finite volume method. *Journal of Hydraulic Research* 2005; **43**(4):376–389.
11. Harten A, Lax PD, van Leer B. On upstream differencing and Godunov-type schemes for hyperbolic conservation laws. *SIAM Review* 1983; **25**(1):35–61.
12. Liang Q, Borthwick AGL, Stelling G. Simulation of dam-and dyke-break hydrodynamics on dynamically adaptive quad-tree grids. *International Journal for Numerical Methods in Fluids* 2004; **46**:127–162.
13. Toro EF, Spruce M, Speares W. Restoration of the contact surface in the HLL Riemann solver. *Shock Waves* 1994; **4**:25–34.
14. Fraccarollo L, Toro EF. Experimental and numerical assessment of the shallow water model for two-dimension dam-break type problems. *Journal of Hydraulic Research* 1995; **33**(6):843–863.
15. Mohamadin A, Le Roux DY, Tajrishi M, Mazaheri K. A mass conservative scheme for simulating shallow flows over variable topographies using unstructured grids. *Advances in Water Resources* 2005; **28**:523–539.
16. Lai JS, Lin GF, Guo WD. An upstream flux-splitting finite-volume scheme for 2D shallow water equations. *International Journal for Numerical Methods in Fluids* 2005; **48**:1149–1174.

DOI: 10.1002/fld

17. Zoppou C, Roberts S. Explicit schemes for dam-break simulations. *Journal of Hydraulic Engineering* 2003; **129**(1):11–34.
18. Erduran KS, Kutija V, Hewett CJM. Performance of finite volume solution to the shallow water equations with shock-capturing schemes. *International Journal for Numerical Methods in Fluids* 2002; **40**:1237–1273.
19. van Leer B. Towards the ultimate conservative difference scheme IV: a new approach to numerical convection. *Journal of Computational Physics* 1977; **23**:276.
20. van Leer B. Towards the ultimate conservative difference scheme V: a second order sequel to Godunov's method. *Journal of Computational Physics* 1979; **32**:101.
21. Toro EF. A weighted average flux method for hyperbolic conservation laws. *Proceedings of the Royal Society of London* (*A*), vol. 423, 1989; 401–418.
22. Li J, Chen G. The generalized Riemann problem method for the shallow water equations with bottom topography. *International Journal for Numerical Methods in Engineering* 2005; **65**(6):834–862.
23. Birman A, Falcovitz J. Application of the GRP scheme to open channel flow equations. *Journal of Computational Physics* 2007; **222**(1):131–154.
24. Colella P, Woodward P. The piece-wise parabolic method (PPM) for gas dynamic simulations. *Journal of Computational Physics* 1984; **54**:174–201.
25. Zhou JG, Causon DM, Mingham CG, Ingram DM. The surface gradient method for the treatment of source terms in the shallow water equations. *Journal of Computational Physics* 2001; **168**:1–25.
26. Nujic M. Efficient implementation of non-oscillatory scheme for the computation of free surface flows. *Journal of Hydraulic Research* 1995; **33**:101–111.
27. Namin M, Lin B, Falconer RA. Modelling esturine and coastal flows using an unstructured triangular finite volume algorithm. *Advances in Water Resources* 2004; **27**:1179–1197.
28. Mohammadian A, Le Roux DY. Simulation of shallow flows over variable topographies using unstructured grids. *International Journal for Numerical Methods in Fluids* 2006; **52**(5):473–798.
29. Bermudez A, Vazquez ME. Upwind methods for hyperbolic conservation laws with source terms. *Computers and Fluids* 1994; **8**:1049–1071.
30. Vazquez-Cendon ME. Improved treatment of source terms in upwind schemes for the shallow water equations in channels with irregular geometry. *Journal of Computational Physics* 1999; **148**:497–526.
31. Hubbard ME, Navarro PG. Flux difference splitting and the balancing of source term and flux gradients. *Journal of Computational Physics* 2000; **165**:89–125.
32. LeVeque RJ. Balancing source terms and flux gradients in high-resolution Godunov methods: the quasi-steady wave-propagation algorithm. *Journal of Computational Physics* 1998; **146**:346–365.
33. Rogers BD, Fujihara M, Borthwick AGL. Adaptive Q-tree Godunov-type scheme for shallow water equations. *International Journal for Numerical Methods in Fluids* 2001; **35**:247–280.
34. Rogers BD, Borthwick AGL, Taylor PH. Mathematical balancing of flux gradient and source terms prior to using Roe's approximate Riemann solver. *Journal of Computational Physics* 2003; **192**(2):422–451.
35. Valiani A, Begnudelli L. Divergence form for bed slope source term in shallow water equations. *Journal of Hydraulic Engineering* 2006; **132**(7):652–665.
36. Marche F, Bonneton P, Fabrie P, Seguin N. Evaluation of well-balanced bore-capturing schemes for 2D wetting and drying processes. *International Journal for Numerical Methods in Fluids* 2006; **53**(5):867–894.
37. Murillo J, Navarro PG, Burguete J, Brufau P. The influence of source terms on stability, accuracy and conservation in two-dimensional shallow flow simulation using triangular finite volumes. *International Journal for Numerical Methods in Fluids* 2007; **54**(5):543–590. Published online: 16 January 2007 (articles online in advance of print).
38. Godunov SK. A finite-difference method for the numerical computation of discontinuous solutions of the equations of fluid dynamics. *Mathemayicheski Sbornic* 1959; **47**(89):271–306 (English translation available in U.S. Joint Publications Research Service [1969]. JPRS 7226).
39. van Leer B. Towards the ultimate conservative difference scheme, I. The quest of monotonicity. *Lecture Notes in Physics* 1973; **18**:163–168.
40. Boris JP, Book DL. Flux-corrected transport, SHASTA: a fluid transport algorithm that works. *Journal of Computational Physics* 1973; **11**(1):38–69.
41. Sweby PK. High resolution schemes using flux limiters for hyperbolic conservation laws. *SIAM Journal on Numerical Analysis* 1984; **21**(5):995–1011.
42. Harten A. High resolution schemes for hyperbolic conservation laws. *Journal of Computational Physics* 1983; **49**(3):357–393.
43. Yu H, Liu YP. A second-order accurate, component-wise TVD scheme for nonlinear, hyperbolic conservation laws. *Journal of Computational Physics* 2001; **173**:1–16.

DOI: 10.1002/fld

44. Lin GF, Lai JS, Guo WD. Finite-volume component-wise TVD schemes for 2D shallow water equations. *Advances in Water Resource* 2003; **26**:861–873.
45. Yoon TH, Kang SK. Finite volume model for tow dimensional shallow water flows on unstructured grids. *Journal of Hydraulic Engineering* 2004; **130**(7):678–688.
46. Goutal N, Maurel F (eds). *Proceeding of 2nd Workshop on Dam-Break Wave Simulation*, France, 1997, HE-43/97/016/B.
47. Mac Donald I, Baines MJ, Nichols NK. Analysis and computation of steady open channel flow using a singular perturbation problems. *Numerical Analysis Report7/97*, University of Reading, 1997.
48. Delis AI, Skeels CP. TDV Schemes for open channel flow. *International Journal for Numerical Methods in Fluids* 1998; **26**:791–809.

DOI: 10.1002/fld